Characterization of Inertial Electrostatic Confinement Fusion Plasma Device

G. M. Elaragi[1], W. E. Madcour[1], Abdel monsef A. El hadary[1], H. M. Abu − zied[2], S. M. Talaat [2] and H. S. Elaraby[1]

1. Plasma Physics and Nuclear Fusion Department, Egyptian Atomic Energy, Cairo, Egypt

2. Physics Department, Women Faculty for Arts, Science, and Education, Ain -Shams University, Cairo, Egypt

elaragi@gmail.com

Abstract

Inertial electrostatic confinement fusion (IECF) device, constructed at the Egyptian Atomic Energy Authority (EAEA-IEC), is introduced the characterization of IEC Plasma Device. The X-ray and visible light emissions in IEC plasma device were investigated by employing time-resolved detector and measure of the total "amount" of visible light using a lux meter.

Keywords: Nuclear Fusion, Plasma Devices, Electrostatic, Confinement, X-Ray

Introduction

The Inertial Electrostatic Confinement (IEC) style of device proves to be a worthy candidate due to its simplicity. The Inertial Electrostatic Confinement plasma devices are interesting way of generating plasmas at high temperatures and have been investigated in the past with special respect to fusion plasma [1-2]. Fusion related applications were also investigated with respect to the development of electric propulsion systems [3-4]; non-fusion systems involved the use of IEC Plasma devices for technical applications for surface modification and as neutron or x-ray sources [5-6]. A Neutron/Gamma-ray combined inspection system for hidden special nuclear materials (SNMs) in cargo containers has been developed in Japan. The inertial electrostatic confinement fusion device has been adopted as neutron source have been developed to realize the fast screening system. The prototype system has been constructed and tested in the Reactor Research Institute, Kyoto University [7]. The IEC fusion device basically consists of a spherical-gridded cathode concentrically placed at the center of a spherical anode filled with a fuel gas. A glow discharge takes place between these electrodes. The produced ions are then accelerated toward the center through the transparent gridded cathode undergoing fusion reactions. An important advantage of IEC over accelerator-driven neutron generators employing solid targets comes from the use of "gas target" or "plasma target. For instance, an IEC neutron generator [8] demonstrated to produce $10^6 - 10^8$ neutrons/sec for D-D fusion. The IEC devices can produce many types of electromagnetic radiation with a wide spectrum. Among them, the most encountered spectrum consists of x-rays, visible infrared, ultraviolet, microwave and gamma rays [12].

Experimental Set-Up

Plasma Inertial Electrostatic Confinement (IEC) is created between two concentric electrodes at low pressure and high voltage, a steady glow discharge is formed. The electrodes consist of stainless-steel wire structures creating relatively homogeneous electric field. Ions are accelerated towards the inner cathode, penetrating the wire structure, collide with each other in the center, and create the high temperature plasma by converting their kinetic energy into thermal energy.

The laboratory experimental set-up of the IEC plasma device is as shown in Figure 1. The IEC is a 10cm of diameter Pyrex glass tube vacuum vessel mounted on a laboratory table. A chamber base pressure of $\sim 10^{-2}$ Torr is achieved using differential pumping. The IEC cathode grid was constructed using stainless steel wire of 1 mm in diameter. High voltage insulation is provided using ceramic feed through system that is extended into the center of the chamber and attached to the cathode grid.

The diameter of the outer electrode was kept constant at the maximum diameter allowed by the chamber dimensions of 10 cm. Inner electrode diameter of 2 cm was tested under similar conditions and the brightness of the plasma inside the inner electrode was chosen as optimization criterion. The outer electrode was made from stainless steel 2mm diameter wire, as inner electrode, conventional steel springs were used and cut to length. For the recent version 1 mm stainless steel wire was used to manufacture the inner electrodes due to the possibility of creating customized electrodes.

Hydrogen gas is injected into the quartz tube through the mass flow controller to regulate the mass flow rate of the propellant gas. The typical operating pressure is 0.08 – 1.0 Torr for Hydrogen gas. If the vacuum vessel has been opened recently, there are surface contaminants, water vapor, grease and other impurities inside the vessel. It takes about 20-30 minutes after the initiation of the discharge during which chamber conditioning and surface cleaning takes place, and the impurities are pumped out of the system. To avoid vapor from back streaming, the vacuum chamber is washed by gas after evacuation by the rotary pump.

Instead of the traditionally used pure DC mode, a rectified AC approach was chosen. Preliminary data indicates that a more stable operational behavior is achieved with the potential to extend the operational range, and arcing was significantly reduced in this operational mode. The resulting output voltage was rectified through a custom-built high voltage diode circuit to maintain the electrode bias with the inner electrode being the negative pole (cathode) and the outer electrode working as the anode at ground potential. The resulting output signal oscillating with 120 Hz as illustrated in Figure 2 was supplied to the IEC. Quasi-stationary IEC plasma fluctuating with a frequency of 120 Hz was obtained for a wide variety of pressures and voltages.
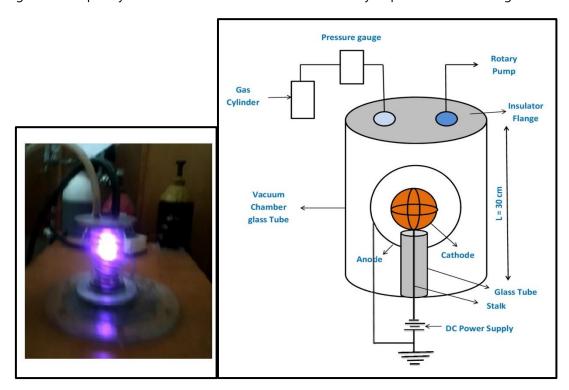

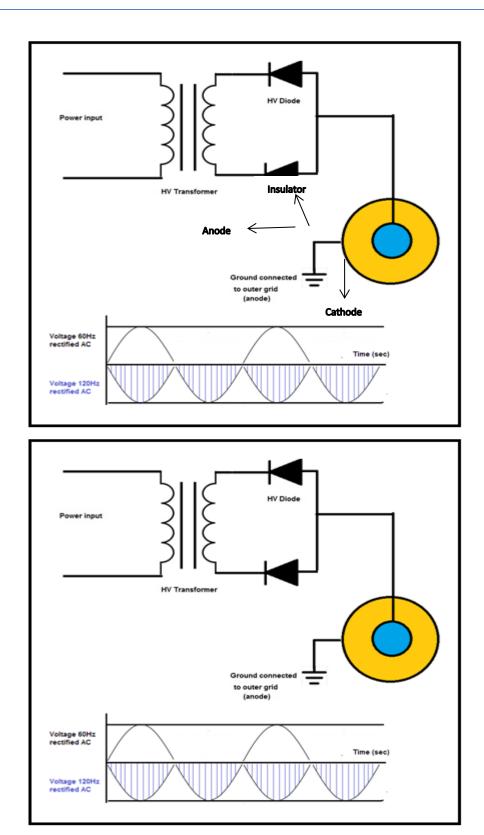Figure 1. Schematic diagram and photo of experimental setup.

Figure 2. Electrical circuit and illustration of the 120 Hz rectified AC voltage supplied to the IEC.

Theoretical Model

A model consisting of *a core surrounded by co-central zones* (CCZ model) is proposed to estimate the ion flux density. The model assumes that the ion beam cross-section consists of a main core of highest density surrounded by several co-central zones of virtual anode and virtual cathode lower densities (figure 3).
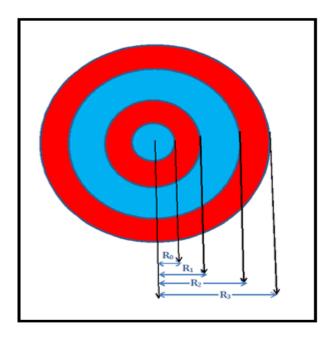

Figure 3. Schematic diagram of the CCZ model

The number of ions inside a predefined small area δ is the first counted for the core and each zone of virtual anode. The total number of ions N_i inside the core and co-central zones is given by

$$N_i = \pi R_0^2 \frac{n_{i0}}{\delta_0} + \sum_{k=1}^{n}(R_k - R_{k-1})2\pi R_k \frac{n_{ik}}{\delta_k} \qquad (1)$$

Where n_{i0} is the number of ions inside a small area δ_0 of the core, n_{ik} is the number of deuterons inside virtual anode of the kth zone, R_0 is the radius of the core, R_1 is the radius of the first zone, R_2 is the radius of the second zone, R_3 is the radius of the three zone, R_k is the radius of the kth zone and k is the number of zones and n is even number.

$$N_i = \pi R_0^2 \frac{n_{i0}}{\delta_0} + (R_2 - R_1)2\pi R_2 \frac{n_{i2}}{\delta_2} + (R_4 - R_3)2\pi R_4 \frac{n_{i4}}{\delta_4} + \text{.......} \quad (2)$$

The total number of electrons N_e inside co-central zones of virtual cathode is given by

$$N_e = \sum_{k=1}^{n}(R_k - R_{k-1})2\pi R_k \frac{n_{ek}}{\delta_k} \qquad (3)$$

Where n_{ek} is the number of electrons inside virtual cathode of the kth zone, R_k is the radius of the kth zone and k is the number of zones and n is odd number.

$$N_e = (R_1 - R_0)2\pi R_1 \frac{n_{e1}}{\delta_1} + (R_3 - R_2)2\pi R_3 \frac{n_{e3}}{\delta_3} + \text{.......} \quad (4)$$

When hydrogen is used, ions produced in the discharge are extracted from the plasma by the cathode grid, accelerated, and focused in the center. The grid provides recirculation of ions, increasing the ion density. Consequently a very high-density core of fuel ions is created in the center region (figure 4). This might enhance fusion reactions, since the reaction rate is proportional to the square of the fuel density. Nevertheless, the high

density of ions produces a high potential spike, which decreases the kinetic energy of incoming ions and consequently reduces fusion reactions.
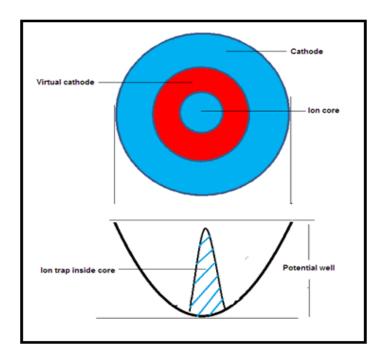

Figure 4. Inertial-Electrostatic Confinement

Ions are accelerated by the cathode and pass through the cathode region towards the center. They are arrived at the central region and then turn back to the cathode region, and reflected again towards the center (figure 5). The spherical symmetry of the electrostatic field near the cathode region is, however, incomplete because the cathode has a discrete structure. This non-symmetric electric field near the cathode region gives the ion beam a certain divergence. In an experiment at high currents, a potential structure develops in the non-neutral plasma, creating virtual electrodes that further enhance ion containment and recirculation [9-10]. The inward and outward motion of the ions is called ''recirculation.'' As they recirculate, ions scatter from each other (arrows in figure 5). While recirculating, a very small fraction of the ions will collide and fuse with background gas (beam-target model). The majority of fusion reactions are beam-background, that is, between the fast moving deuterons in the plasma and the neutral background gas. Since there is no solid target upon which ions are directed there is no a solid target that will deteriorate from plasma interactions. Hirsch [11] pointed out firstly an existence of the potential well or a virtual cathode structure in the potential spike. Each ion accelerates on its trips toward the center and decelerates on its trips away from center. Their energies at the edge of the well are small compared with their energies at center. At the center the ions have enough energy to have a substantial probability for fusing. Individual ions oscillate in the electrostatic well, and fusion reactions then occur from high-energy collisions between the counter streaming ions or with background neutral particles. The beam number fluency (ρ_{ion}) of an ion core beam is given by

$$\boldsymbol{\rho_{ion} = \frac{N_{deuteron}}{A_{beam}}} \qquad (5)$$

Where A_{beam} is the area covered by the ion beams in m^2.According to CCZ model, it is possible to estimate the total number of ions inside core. For instance, let the total cross-sectional area of core sphere is $\sim \boldsymbol{1.13 \times 10^{-6}\ m^2}$. The estimated total number of ions is equal to 10^3-10^5 ions. The beam number fluency (using eq. (5)) is $8.8 \times 10^9 - 10^{11}$ ions/m^2 and ion density $\cong \boldsymbol{10^{13} - 10^{15}\ ions/m^3}$.

Beam flux= beam number fluency × pulse duration (0.5μs) = 4400 ions/m^{2}s
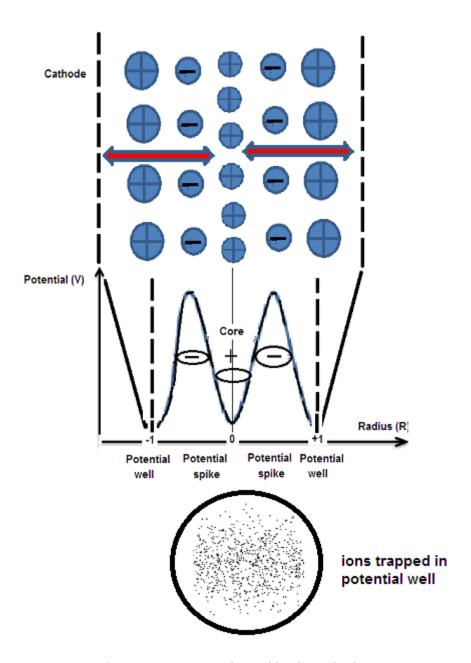
Figure 5. Ions are accelerated by the cathode

Results and Discussion

The applied voltage and the discharge current through the discharge chamber were measured using a voltage divider (homemade), which was connected between the two electrodes, and a current monitor, which can be located upon returning to the ground. The signals from the voltage divider and the current monitor were recorded in a digitizing oscilloscope (Lecroy, USA) with 200 MHz bandwidth. Figures 6 and 7 indicate the current waveforms characterizing the pulsed IEC fusion device for different gases (air and hydrogen respectively).

Figure 8 shows the relation between discharge current, in mA versus the discharge voltage, in kV using hydrogen gas. It is clear that the discharge current increases by increasing the
discharge voltage. At higher voltages more electrons are extracted from the cathode surface per unit area and the current increases.
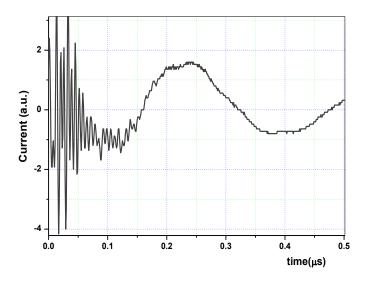
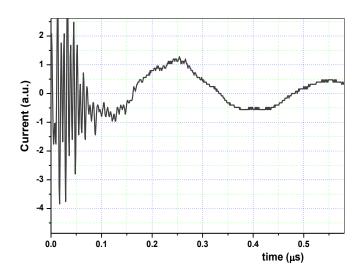Figure 6. Discharge current signal from air plasma

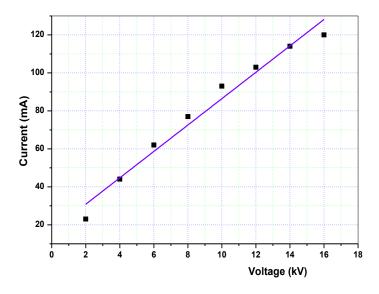
Figure 7. Discharge current signal from hydrogen plasma

Figure 8. The relation between discharge voltage and discharge
current for IEC plasma device

Figure 9 indicate photographs of air plasma at different pressures. Figure 10 show the effectiveness of IEC glow discharge, for illuminance (visible flux density) emitted from air and hydrogen plasmas at low pressures investigated. The illuminance with the gas pressure increased exponential, due to the characteristics of IEC at the low pressures to produce more energetic excitation. At low pressure, the mean free path of electron is large. Then electrons gain a lot of energy from the applied electric field to create more excitations and ionizations through inelastic collisions with others plasma particles. Consequently during emission transitions and recombination of electrons with the ions, the illuminance will be increased and tend to increase with the increasing pressure. Illuminance is measured using an instrument known as light-meter [Model LX-101A].
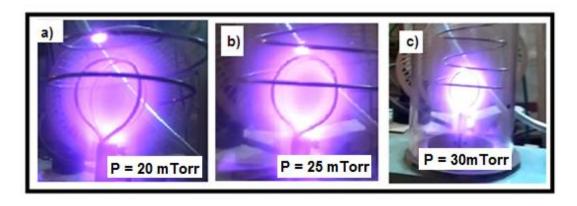

Figure 9. An exemplary for change air glow characteristics over pressure at constant voltage level.
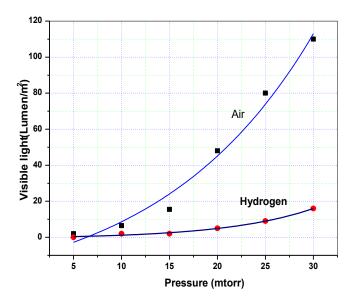
Figure 10. Illuminance of visible light as a function of pressure for glow air and hydrogen plasmas

Hydrogen gas is substituted for deuterium because in this configuration the main function of gas ions is to provide electron Bremsstrahlung emission. A scintillator photomultiplier tube (SPMT) assembly was employed for the detection of hard X-ray, which was placed at a distance a few centimeters away from the evacuated chamber. The scope graph below (Figure 11) is from the experiment of IEC plasma device when hydrogen is the working gas.

X-rays are produced when high energy electrons strike high-atomic-number targets. Electrons coming from the inner grid and hitting outer grid wires would be possible sources. Colliding high-energy ions can also release essentially identical radiation. Electrical discharges in hydrogen gas are commonly used to produce ultraviolet radiation at short wavelengths. Fortunately, it doesn't penetrate glass chamber very well.
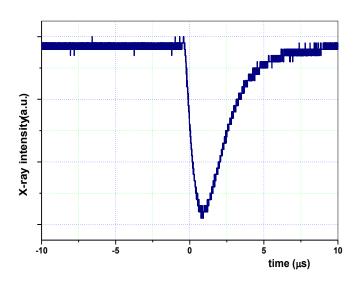

Figure 11. Signal of scintillation hard X-ray detector for hydrogen plasma

Conclusion

The power supply used in the experiment not pure DC mode. The output voltage oscillating with 120 Hz was supplied to the IEC device. Theoretical model called core surrounded by co-central zones (CCZ model) was proposed to estimate ion density of fuel ions created in the center region. The discharge current is two to three orders more in the case of air plasma than hydrogen plasma discharge. The flux density of visible light emitted from air and hydrogen plasmas for different pressures was investigated. At pressure 20 m Torr, visible flux density of air glow plasma is more than 9.6 times hydrogen visible glow.

Reference

1.   Messier, Douglas. "Tiny 'Cubesats' Gaining Bigger Role in Space". Space.com. Retrieved 23-5 (2015).

2.   G. R. Piefer, John F. Santarius, Robert P. Ashley, Gerald L. Kulcinski, "Design of an Ion Source for 3He Fusion in a Low-Pressure IEC Device", Fusion Science and Technology 47, 1255-1259 (2005).

3.   G.H. Miley et al., Inertial Electrostatic Confinement as a Power Source for Electric Propulsion. Proceedings of the NASA Vision-21 Conference, NASA Lewis Research Center, Cleveland, OH, 30-31 March (1993).

4.   R.W. Bussard and L.W. Jameson, Inertial-Electrostatic-Fusion Propulsion Spectrum: Air-Breathing to Interstellar Flight. Journal of Propulsion and Power, 11:365-372, March-April (1995).

5.   G. H. Miley, L. Wu, H. J. Kim, "IEC-based neutron generator for security inspection system", Journal of Radioanalytical and Nuclear Chemistry 263, 1, 159-164 (2005).

6.   Y. GU and G.H. Miley, Spherical IEC Device as a Tunable X-Ray Source. Bulletin of the American Physical Society: 40:1851, (1995)

7.   H. Ohgaki, Member, IEEE, I. Daito, H. Zen, T. Kii, K. Masuda, T. Misawa, R. Hajima, T. Hayakawa, T. Shizuma, M. Kando, and S. Fujimoto "Nondestructive Inspection System for Special Nuclear Material Using Inertial Electrostatic Confinement Fusion Neutrons and Laser Compton Scattering Gamma-rays" IEEE Transactions on Nuclear Science (Volume: 64, Issue: 7, July 2017)

8.   G.M.EL-ARAGI, "Building Inertial Electrostatic Confinement Fusion Device Aimed for a small Neutron Source", International Journal of High Energy Physics, 4(6):88-92, (2017).

9.   G.M.EL-ARAGI, "Operation of Inertial Electrostatic Confinement Fusion (IECF) Device using different gases" Journal of Fusion Energy Vol. 37, Issue 1, pp 37-44, (2018)

10.   G. H. Miley, et al., "Discharge Characteristics of the Spherical Inertial Electrostatic Confinement (IEC) Device," IEEE Trans, on Plasma Science, 25, 4, 733-739, (1997)

11.   George H. Miley and Yibin GU, "IEC Neutron Source Development and Potential Well Measurements," Current Trends in International Fusion Research, E. Panarella, ed., NRC Press, Canada, (1999).

12.   HIRSCH, R.L.J. Appl. Physics 38, 4522 (1969)

13.   Matsuura H, Takaki T, Funakoshi K, Nakao Y, Kudo K. Ion distribution function and radial profile of neutron production rate in spherical inertial electrostatic confinement plasmas. Nucl Fusion; 40(12):1951-4 (2000).